Biochemistry and Biophysics Reports 40 (2024) 101817

Contents lists available at ScienceDirect

Biochemistry and Biophysics Reports

journal homepage: www.elsevier.com/locate/bbrep

New findings on the orientation of the mouse anterior-posterior (A-P) axis before and during the initiation of gastrulation using a more refined embryo staging

Xenia Hadjikypri [1], Christina Theofanous [1], Antonia Christodoulidi, Pantelis Georgiades [*]

Department of Biological Sciences, University of Cyprus, University Campus, P.O. Box 20537, 1678, Nicosia, Cyprus

ARTICLE INFO

Keywords:
Anterior-posterior axis orientation
Mouse
Pre-gastrulation embryo
Embryo staging
Bilateral symmetry

ABSTRACT

A clinically significant event of early mammalian embryogenesis is the generation and early development of the anterior-posterior (A-P) axis, the imaginary line along which the structures from head to tail will form. This axis not only appears before gastrulation but is also oriented in a specific way in relation to the long and short diameters of the bilaterally symmetric epiblast. In mice, the most widely used mammalian *in vivo* model of early embryogenesis, the A-P axis is normally aligned with the long epiblast diameter by the early streak (ES) stage, a time during early gastrulation around embryonic day 6.5 (E6.5). Incorrect orientation of the A-P axis by the ES stage, that is, being aligned with the short epiblast diameter, leads to failure in completing gastrulation and results in embryo death soon after. Knowing the orientation of this axis from when it forms before gastrulation (around E5.5) until just before the ES stage is crucial for: (a) understanding the ill-defined factors involved in its formation and early development since they must be spatially related to it, and (b) providing explanations for the underlying mechanism when it is incorrectly orientated. However, the orientation of the A-P axis in pre-ES embryos of the E5.5-E6.5 period remains unclear. Specifically, although it is thought that this axis initially aligns with the short epiblast diameter and subsequently changes its orientation to become aligned with the long diameter by an unidentified pre-gastrulation stage before the ES stage, this proposition remains unresolved. This is largely due to the lack of clearly defined morphological criteria for staging certain periods of pre-ES mouse embryos (especially when the A-P axis initiates and when gastrulation begins prior to the ES stage), which are a prerequisite for identifying A-P axis orientation at specific pre-ES stages. Furthermore, although the orientation of an extraembryonic trophoblast asymmetry, specifically the tilt of the ectoplacental cone (EPC), coincides with that of the A-P axis by the ES stage, it is unknown whether such an association also exists at pre-gastrulation stages during A-P axis formation. Knowing this would exclude or implicate this trophoblast asymmetry as an upstream factor in orientating the A-P axis when it forms. To address these issues, we established a more refined embryo staging for the E5.5-E6.5 period using a novel combination of live morphological criteria and used it to examine the orientation of the A-P axis and that of the EPC tilt at specific stages. First, contrary to current thinking, we show that when the A-P axis first appears at our newly described anterior visceral endoderm-1 (AVE-1) and AVE-2 stages, it aligns with the long epiblast diameter in all embryos. This orientation is maintained in most embryos at all subsequent pre-gastrulation stages, specifically at our AVE-3 and pre-streak stages (the remaining embryos of these stages had this axis aligned with the short epiblast diameter). Second, we identified for the first time the pre-ES stage when gastrulation initiates, which we named the nascent streak (NS) stage, and further subdivided it into NS-1 and NS-2. At variance with current belief, we provide evidence that the earliest stage just before the ES stage when all embryos align their A-P axis with the long epiblast diameter is not a pre-gastrulation stage, but the NS-2 stage (at NS-1, most but not all embryos had this A-P axis orientation). Third, we implicate the EPC tilt as a possible extraembryonic factor in promoting correct A-P axis orientation, as this tilt exists before the AVE-1 stage and its orientation coincided with that of the A-P axis in all embryos at AVE-1, AVE-2 and ES stages and almost all embryos at AVE-3, pre-streak and NS stages. Overall, our work: (a) identified the previously unresolved orientation of the mouse A-P axis within the epiblast before the ES stage during the E5.5-E6.5 period; (b) provides an alternative explanation for when this axis is incorrectly oriented by

* Corresponding author.
E-mail address: pgeor@ucy.ac.cy (P. Georgiades).
[1] *Co-first authors* (contributed equally to this work).

https://doi.org/10.1016/j.bbrep.2024.101817
Received 24 June 2024; Received in revised form 11 August 2024; Accepted 25 August 2024
Available online 29 August 2024

the ES stage, namely, its defective alignment with the short epiblast diameter by this stage could be due to its failure to align with the long epiblast diameter from the time of its formation; and (c) implicates the pre-existing orientation of the EPC tilt as a possible factor in orientating the newly formed A-P axis.

1. Introduction

The anterior-posterior (A-P) axis is an imaginary line that passes through the centre of the adult body or embryo, along which the different structures or cell types (asymmetries) that exist between the head and tail are found. The mammalian A-P axis is the first definitive body axis to form during early embryogenesis and leads to the establishment of the dorsoventral (D-V) and left-right (L-R) body axes, which collectively define the basic body plan, the spatial blueprint of the newborn. The early development of the A-P axis occurs within the epiblast, the one cell-thick epithelium progenitor of the new-born. This axis initiates before the formation of the primitive streak, a transient structure that marks the posterior end of this axis and signifies the beginning of gastrulation. The earliest indications of A-P axis formation are molecular asymmetries in the epiblast along the imaginary line that defines this axis [1–3]. Early A-P axis development in eutherian mammals (e.g., mice and humans) has been extensively studied in the mouse embryo, the most widely used *in vivo* model for early human embryogenesis, as access to human embryos during this period is hampered by ethical, legal and technical limitations [4,5]. In mice, the A-P axis initiates at approximately embryonic day 5.5 (E5.5) and the earliest formation of mesoderm, the first derivative of the primitive streak which signifies that gastrulation is under way, occurs at around E6.5, at the early streak (ES) stage [1–3,6].

Important parameters for understanding early A-P axis development include knowledge of the geometrical shape and symmetry of the epiblast, as well as the orientation of this axis in relation to these. Before and during A-P axis formation in eutherian mammals, irrespective of the epiblast's overall three-dimensional shape (that is, flat as in humans, rabbits, pigs and cattle, or cup-shaped as in mice), its geometrical shape is ellipsoid (resembles a 'squashed' circle). Consequently, the eutherian epiblast during this period is bilaterally symmetric, as it has at least one axis of reflection symmetry: imaginary line that divides a two-dimensional object (e.g., ellipsoid epiblast epithelium) or a plane through a three-dimensional object (e.g., foetus/new-born), into two mirror-image halves. Just before A-P axis formation, the eutherian epiblast is bilaterally symmetric with two axes of reflection symmetry (a long and a short one that pass through the centre of the epiblast and are at right angles to each other), which define its long and short diameters. Once the A-P axis has formed however, although these two epiblast diameters still exist, the bilaterally symmetric epiblast only has one axis of reflection symmetry. This is due to A-P axis formation being a symmetry breaking event because the imaginary line along which the asymmetries that define the newly formed A-P axis are arranged, coincides with one of the two initial axes of reflection symmetry or epiblast diameters [7–16]. Although the ellipsoid shape of the epiblast can be easily discerned in embryos with a flat epiblast, this geometry in the cup-shaped mouse epiblast can be visualized in two ways. The first is when the intact cup-shaped epiblast is mentally flattened out (after a virtual 'opening up' of the cup by a virtual 'pull-down' of its 'lips'), since the area and perimeter of the 'flattened' epiblast are those of an ellipse [10]. The second is when the epiblast is sectioned at the mid-level of the proamniotic cavity along the proximo-distal (P-D) axis (proximal and distal ends of the P-D axis are the lips and base of the cup, respectively) with the plane of sectioning being perpendicular to this axis. This is because the perimeter of the resultant section is that of an ellipse [7]. Extrapolating from this, the long and short epiblast diameters can be identified directly in intact live mouse embryos before or after A-P axis formation. Specifically, the long epiblast diameter is the longest imaginary line found at a specific embryo orientation (after rotation around its P-D axis) that is perpendicular to the P-D axis, passes through the mid-level of the proamniotic cavity and connects the two opposite outer edges of the cup-shaped epiblast at this level [7,17]. Conversely, the short epiblast diameter is the line detected using the criteria defined above but after a 90° rotation from its long epiblast diameter orientation [7,17].

The first of the two main topics we investigated was the unresolved orientation of the mouse A-P axis within the epiblast in pre-ES stages, that is, whether it is aligned with the long or short epiblast diameters from when it first forms before gastrulation. However, the orientation of the mouse A-P axis from the ES stage onwards is well established: it aligns with the long epiblast diameter [8,15], as is the case for all other eutherian mammals examined, including humans [9–14]. Knowledge of A-P axis orientation from when it first forms before gastrulation, is crucial for several reasons including the following. Incorrectly oriented A-P axis by the ES stage, that is, having it aligned with the short rather than the long epiblast diameter, is associated with failure to complete gastrulation and embryo death soon after [18–21]. Defective A-P axis orientation as a cause of abnormal gastrulation and embryo death soon after gastrulation initiation may be clinically relevant to early unexplained miscarriage, the most common post-implantation pregnancy complication. It is estimated that 30 % of human embryos that implant die soon after the onset of gastrulation, that is, between the end of the second week after fertilization (gastrulation initiation) and the sixth week [5] and most of these (about 70 %) have morphological defects consistent with failure of gastrulation [22]. Knowing the orientation of the A-P axis from when it first forms, is important for elucidating the ill-defined signals that promote its formation and early development, since they must be spatially related to its orientation. Learning about the orientation of the mouse A-P axis before gastrulation is a prerequisite for determining whether the mouse embryo is a valid *in vivo* model for studying early A-P axis development in humans. Although this presupposes that pre-gastrulation A-P axis orientation is similar in both mice and humans, this is orientation is known in humans but remains unclear in mice. Specifically, all non-mouse eutherian mammals studied, including humans, have their A-P axis aligned with the long epiblast diameter from the time of its formation before gastrulation and at all subsequent stages [9–14]. However, in mice, the pre-ES stage orientation of this axis is still unresolved, as interpretation of published findings about this needs further investigation. The published interpretation posits that, unlike other eutherian mammals, the mouse A-P axis is initially aligned with the short epiblast diameter from the time of its formation prior to gastrulation until an undefined stage just before the ES stage, by which time it becomes aligned with the long epiblast diameter due to epiblast reshaping [2,7,15,16,17]. Here we experimentally challenged the validity of this interpretation in three ways that are discussed in the three paragraphs that follow.

The first unresolved issue we investigated in relation to the orientation of the A-P axis within the epiblast was its unknown orientation when it first forms between E5.5 and E5.75. This is because the embryonic stage when this axis initiates, which is a prerequisite for identifying its orientation when it first appears, is still undetermined. The reason is that current staging is not informative about the earliest stages of the period during which laterodistal visceral endoderm thickening (laterodistal VET) exists. Laterodistal VET is a transient VE structure that exists from E5.5 to E5.75, whose appearance coincides with that of the A-P axis within the epiblast [2,17]. Specifically, there are no clear live morphological criteria for identifying the anterior and posterior limits of laterodistal VET and their P-D location, both important parameters for subdividing the laterodistal VET period into stages, since this VET

progressively moves proximally [17,23,24]. The interpretation that mouse embryos initially align their A-P axis with the short epiblast diameter [2,17] was deduced from the finding that most embryos with ellipsoid epiblast (about 60 %) that were examined during the laterodistal VET period, had their A-P axis aligned with the short epiblast diameter, whilst in the remaining (approximately 40 %) it was aligned with the long diameter [17]. However, a different interpretation that is also consistent with these results, and which was tested here, could be reached if the embryos examined: (a) were staged using a more refined embryo staging that subdivides the laterodistal VET period into early and late stages, and (b) were all embryos with a laterodistal VET since the aforementioned study excluded those with an 'extremely bent ectoplacental cone' [17]. This alternative interpretation is that the A-P axis is aligned with the long epiblast diameter in all embryos at the earliest stages of the laterodistal VET period and with most embryos at each of the later stages (the remaining minority align it with the short diameter). Therefore, to identify the elusive orientation of this axis when it first forms and at the immediate stages that follow, we aimed to establish novel morphological criteria for subdividing the laterodistal VET period into two or more stages and identify A-P axis orientation at these new stages.

The second unknown that was examined here regarding A-P axis orientation within the epiblast was its undetermined orientation between E6.0 and E6.5 in pre-ES embryos after the laterodistal VET period. Even though it is thought that the least developmentally advanced embryos of this period have their A-P axis aligned with the short epiblast diameter and the more advanced ones with the long epiblast diameter [2,7,16], the validity of this claim remains elusive. This is because there are no clearly defined live morphological criteria for staging embryos of this period [23,24], an essential requirement for comparing A-P axis orientation between early and late stages of this period. This interpretation was deduced from the finding that most pre-ES embryos of the E6.0-E6.5 period that were presumed to be the least developmentally advanced, had their A-P axis aligned with the short epiblast diameter [7,16]. However, these investigators judged the degree of developmental advancement in embryos of this period based on two unreliable criteria. The first was chronological embryo age [7] (estimated amount of time elapsed since fertilization), which is not an accurate indicator of the extent of developmental progression [6]. The second was the P-D length of the egg cylinder, that is, the combined P-D length of the embryonic region [epiblast and its associated VE (embryonic VE)] and that of the extraembryonic region [extraembryonic ectoderm (ExE) trophoblast and its associated VE (extraembryonic VE)] [16]. However, the assumption that a longer egg cylinder length during the E6.0-E6.5 period reflects more advanced stages [16] may not be a reliable staging criterion because considerable overlap in this length was reported between pre-ES and ES E6.5 embryos [6]. Therefore, we aimed to establish novel morphological criteria for staging post-laterodistal VET embryos prior to the ES stage during the E6.0 to E6.5 period and use it to identify A-P axis orientation at each of these new stages for the purposes of testing an alternative hypothesis: each of the least advanced stages of this period contain embryos with both A-P axis orientations, most of whom have this axis aligned with the long epiblast diameter.

The last unknown that we addressed about A-P axis orientation within the epiblast is as follows. Although it is well-known that all embryos align their A-P axis with the long epiblast diameter by the ES stage [2,7,15,16], whether the earliest stage when this occurs is before or during gastrulation, as well as the identity of this stage, are open questions. The current belief that the earliest stage closest to the ES stage when all embryos have their A-P axis aligned with the long epiblast diameter is a pre-gastrulation one, was based on the finding that this type of A-P axis orientation was observed in pre-mesoderm embryos just before the mesoderm-containing ES stage [2,7,15,16]. However, not all pre-mesoderm embryos belong to pre-gastrulation stages because gastrulation initiates before the appearance of mesoderm, that is, just before the ES stage [6,25–27]. Specifically, although the primitive streak, which signifies that gastrulation is underway, is usually depicted as epithelial-to-mesenchymal (EMT) epiblast together with sub-adjacent pre-migratory mesoderm that has just exited the epiblast [28], it is well established that gastrulation initiates before mesoderm formation with the appearance of EMT epiblast [6,25–27]. This pre-mesoderm EMT epiblast was detected ultra-structurally [25] and by the pre-mesoderm epiblast expression of *Bra* [26,27]. Surprisingly, current embryo staging systems do not offer any live morphological criteria for clearly identifying the gastrulation initiation stage [6,23,24], which we name 'nascent streak' (NS). Consequently, to address these issues (determining whether the earliest stage closest to the ES stage when all embryos have their A-P axis aligned with the long epiblast diameter is a pre-gastrulation stage or not, as well as identifying this stage), we aimed to establish a more refined embryo staging that identifies the NS stage and the stages immediately preceding it and to examine the orientation of this axis at these new stages.

The second of the two main topics of our work was to investigate the unknown association between the orientation and polarity of the A-P axis and those of a tilt of the ectoplacental cone (EPC), an early extraembryonic trophoblast tissue, from just before of A-P axis formation until the ES stage. We investigated this because: (a) this EPC tilt is present from when EPC forms, a time before A-P axis formation [29] and (b) although the orientation of EPC tilt, but not its polarity, is aligned with that of the A-P axis at the ES stage [15], whether this is the case at earlier stages is unknown [30,31]. Any such association would implicate or exclude for the first time this trophoblast asymmetry in orientating (and possibly also polarizing) the pre-gastrulation A-P axis. The EPC forms around E5.5 from a mesometrially directed growth of the proximal edge of ExE, which itself forms by E5.0. Collectively, EPC and ExE are the progenitors of all placental trophoblasts. The EPC tilt manifests as a tilt in the ExE-EPC border, which coincides with a circumferential constriction of extraembryonic visceral endoderm (exVE) as the latter turns outwards to convert to parietal endoderm [15,29–32]. The orientation of EPC tilt is detectable at the embryo view (after embryo rotation around its P-D axis) where the length of *exVE* (distance between its proximal end which coincides with the ExE-EPC junction and its distal end at the ExE-epiblast border) on one side, is conspicuously different from that on the opposite side. The polarity of this tilt, that is, the direction towards which it is tilted, is the side with the shorter exVE length [30–32]. Since the orientation and polarity of the EPC tilt in relation to those of the A-P axis have not been examined in pre-gastrulation embryos, we investigated this using a more refined embryo staging.

2. Materials and methods

2.1. Embryos, staging, epiblast diameter measurements, determination of A-P axis and EPC tilt orientation/polarity and statistics

Nulliparous females and stud males, three to twelve months old, from wildtype ICR, BALB/c and C57BL/6 strains were maintained under standard conditions (light and dark periods from 6:00–18:00 and 18:00–6:00, respectively) and mated to generate ICR, BALB/c and C57BL/6 embryos according to project licence CY/EXP/PR.L5/2018. All mouse experiments were in accordance with ARRIVE guidelines, the U. K. Animals (Scientific Procedures) Act 1986 and associated guidelines, and EU Directive 2010/63/EU. Embryonic age 0.5 (E0.5) was 12 noon of plug detection day. After Reichert's membrane removal, live embryos with intact egg cylinders were imaged at various orientations upon rotation around their P-D axis, using inverted microscopy (Zeiss Axiovert-200 M or Opto-Edu A14.2603). Embryo staging and identification of the orientation of the A-P axis (relative to the long and short epiblast diameters) and that of the EPC tilt (relative to the orientation of the A-P axis) were carried out using morphological criteria from live embryo imaging. Briefly, embryo staging was accomplished using morphological criteria as described in SupplTable-1 and Suppl.Fig. 1 and shown in

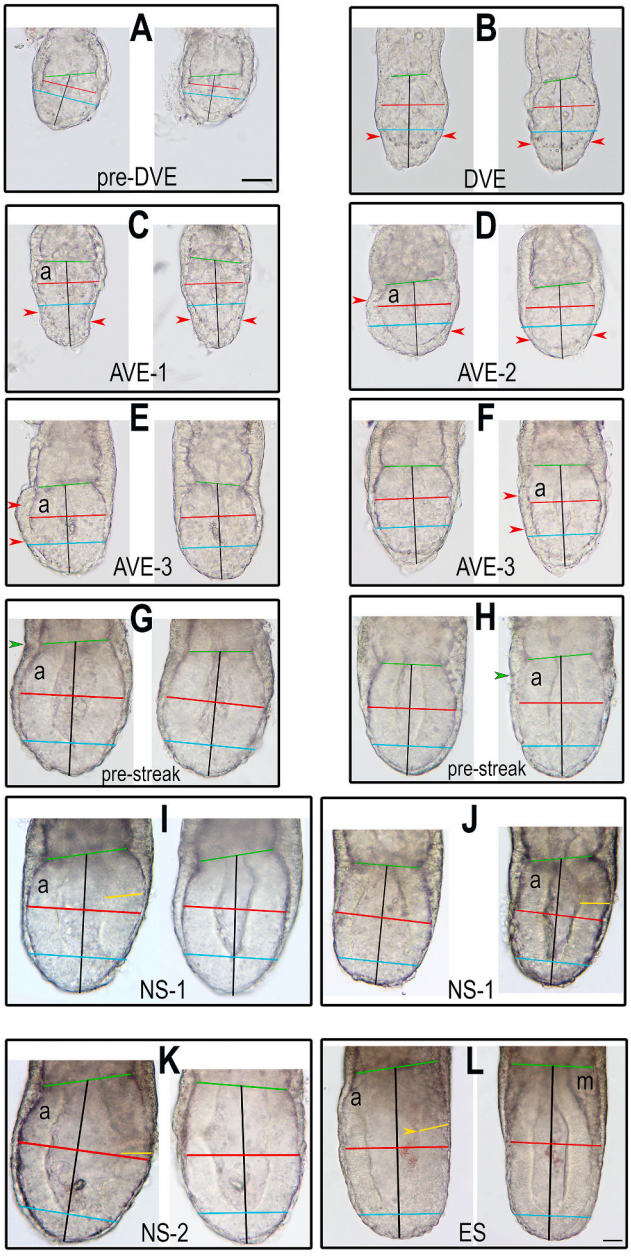

Fig. 1. *A-P axis orientation in relation to the long and short epiblast diameters in live embryos using a more refined staging system for the period between pre-DVE and ES stages*. Each panel shows two live images of same embryo at two orientations after rotation around its 'P-D axis': left and right images coincide with the 'long and short epiblast diameter' sides, respectively. Before and after A-P axis formation (pre-DVE/DVE and AVE-1 to ES stages, respectively) the epiblast is bilaterally symmetric, as it has long and short epiblast diameters (A–L): Once A-P axis forms (detected in 'embryo side views'), it aligns with: (a) long epiblast diameter in AVE-1/2 (C, D), NS-2 (K) and ES (L), and (b) either long or short epiblast diameters in AVE-3 (E and F, respectively), pre-streak (G and H, respectively) and NS-1 (I and J, respectively). For explanation of stages and terms in inverted commas, see main text, Suppl.Fig. 1 and SupplTable-1. Panels A–K are at same magnification (scale bars in A and L are 100 μm). Symbols and letters: green line, 'epiblast-ExE junction'; blue line: 'proximal border of distal tip'; black line, 'P-D axis'; red line, 'epiblast diameter' and 'mid-level of proamniotic cavity'; yellow line, distal-most end of 'asymmetric opacity in proximal embryonic region'; red arrowheads, borders of 'VET'; yellow arrowhead, 'distal end of mesodermal wings'; green arrowheads, 'dent in VE' (anterior side in the vicinity of 'epiblast-EXE junction') in pre-streak embryos; a, anterior end of epiblast (only in embryos with A-P axis); m, 'mesoderm'.

Fig. 1. It was based on the presence or absence of: (a) mesoderm to distinguish the mesoderm-containing ES embryos from pre-ES stages which lack mesoderm (an additional criterion in mesoderm-containing embryos was the location of distal end of mesodermal wings to tell apart ES embryos from more advance stages), (b) asymmetric opacity in the proximal embryonic region, as its presence in pre-ES stages was unique to the NS stage (the location of the distal end of this feature allowed subdivision of NS embryos into NS-1 and NS-2 stages), and (c) visceral endoderm thickening (VET) found in the embryonic VE distal to the mid-level of proamniotic cavity to discriminate between VET-containing embryos (DVE, AVE-1,2,3) and those without it (pre-DVE and all stages from pre-streak onwards). An extra criterion in embryos with such VET was its location to differentiate between DVE, AVE-1, AVE-2 and AVE-3 stages. Identification of the orientation of the A-P axis was according to the morphological criteria described in Table-1 and Suppl.Fig. 1 and shown in Fig. 1. This involved identification of the embryo orientation, after rotation around its P-D axis, where the 'embryo side-view' (orientation were both ends/sides of the A-P axis are morphologically distinguishable and seen at opposite ends in the same embryo image) is detectable, followed by determining whether the embryo side-view is aligned or almost aligned with the embryo orientation that correspond to the long and short epiblast diameters (the latter are explained in the Introduction). If the orientation of the embryo side-view coincided or almost coincided with that of the long or short epiblast diameters, the A-P axis was considered to be aligned with the long or short diameter, respectively. An association between the orientation of the EPC tilt (see Introduction for explanation) was based on using embryos with an intact ExE-EPC border and a conspicuous EPC tilt, as described in Table-1 and Suppl.Fig. 1 and shown in Fig. 3. If the orientation where EPC tilt was conspicuous coincided (or almost coincided) with that of the embryo side-view, the orientation of this tilt was considered aligned with that of the A-P axis. Statistically significant differences between different stages in embryo age and degree of epiblast 'flatness' (% difference between long and short epiblast diameters) were those with $P \leq 0.05$ or ≤ 0.10 using non-parametric Mann-Whitney *U* test.

2.2. Embryo wholemount in situ hybridization (WISH), cryo-sectioning and microsurgery

After live imaging, some embryos were subjected to: (a) WISH for *Bra* and *Cerberus*, either simultaneously for both or each separately, as previously described [33], and (b) microsurgery for separating epiblast, ExE and VE using trypsin/pancreatin digestion as done before [34]. All WISH embryos were imaged at similar orientations as their respective live counterparts (to link live morphology with gene expression) and some cryo-sectioned (to validate presence or absence of mesoderm) as done previously [34], except for the use of ice-cold acetone for snap-freezing and DPX for section mounting.

3. Results and discussion

We first devised a more refined embryo staging from just before A-P axis initiation at around E5.5 [at the well-established pre-distal VE (pre-DVE) and distal VE (DVE) stages] until when mesoderm first appears at the well-defined ES stage at around E6.5 [15,6,17,23,24]. After imaging 164 live embryos (128, 9 and 27 embryos from ICR, BALB/c and C57BL/6 strains, respectively) isolated between E5.4 and E6.9, we used a novel combination of live morphological criteria applicable to all strains that are described in Suppl.Fig. 1 and SupplTable-1. This led to the identification of nine stages shown in Fig. 1 and explained in Suppl. Table-1: pre-DVE, DVE, anterior VE-1 (AVE-1), AVE-2, AVE-3, pre-streak, nascent streak-1 (NS-1), NS-2 and ES. Stages were validated molecularly based on WISH for identifying the expression of *Bra*, marker of EMT epiblast and newly formed mesoderm [26] and *Cer,* marker of DVE/AVE [16]. Positive and negative controls for WISH were the

Table-1

Quantitative data on epiblast bilateral symmetry, A-P axis orientation and polarity in relation to those of EPC tilt and the long and short epiblast diameters in embryos from pre-DVE to ES stages.

For explanation of stages and terms in *underlined italics*, see main text, Suppl.Fig. 1 and SupplTable-1.

	Parameters measured in live embryos (apply to ICR, BALB/c and C57BL/6 stains) Terms in *underlined italics* are explained in Supplementary Fig. 1				
Embryo Stages Staging according to our novel combination of live morphological criteria (for more details, see main text, SuppTable-1, SuppFig. 1 and 1 and 2).	**% of embryos with bilaterally symmetric epiblast**. Having a *bilaterally symmetric epiblast* assumes that each embryo has an *ellipsoid epiblast*: possesses *long and short epiblast diameters*. n = number of embryos inspected.	**% length that long epiblast diameter is longer than the short epiblast diameter in live embryos**. Expressed as mean of this % +/− SEM. P ≤ 0.05) ** or P ≤ 0.10) * denotes statistically significant difference, relative to previous stage using the non-parametric Mann-Whitney *U* test. n = number of embryos measured.	**% of embryos whose anterior-posterior (A–P) axis orientation more aligns with the:** 1. **long epiblast diameter** 2. **short epiblast diameter**. Here we determined whether the *orientation of A-P axis* (which is detectable in *embryo side-views*) coincides or approximately coincides with the embryo orientation where the *long or short epiblast diameters* are detectable. n = number of embryos inspected.	**% of embryos whose ectoplacental cone (EPC) tilt orientation more aligns with the:** 1. **long epiblast diameter** 2. **short epiblast diameter**. Here we determined whether *EPC tilt orientation* aligns or approximately aligns with the embryo orientation where the *long or short epiblast diameters* are detectable. n = number of embryos inspected (only those with relatively intact *ExE-EPC junction* and a conspicuous *EPC tilt*).	**Ectoplacental cone (EPC) tilt orientation and polarity relative to those of anterior-posterior (A–P) axis:** 1. % of embryos whose *EPC tilt orientation* coincides with that of *A-P axis* (the latter detectable in *embryo side-views*). 2. In embryos where *EPC tilt orientation* and *orientation of A-P axis* coincide, what is the **% of embryos** where the **directionality of EPC tilt** (part of *EPC tilt polarity*) is either **towards** the **posterior** or **anterior** ends of *A-P axis* (indicative of *polarity of A-P axis*)? n = number of embryos inspected (only those with relatively intact *ExE-EPC junction* and a conspicuous *EPC tilt*).
Pre-DVE stage (*pre-distal visceral endoderm stage*)	**100 %** n = 5 (4 ICR, 1 C57BL/6)	**10.3 %** ± 1.6 n = 4 (3 ICR, 1 C57BL/6)	**Non-applicable** (there is no known morphological A-P axis)	EPC tilt aligned with: 1. **long** epiblast diameter: **100 %**, n = 4/4 (3 ICR, 1 C57BL/6) 2. **short** epiblast diameter: **0 %**, n = 0/4	**Non-applicable** (there is no known morphological A-P axis)
DVE stage (*distal visceral endoderm stage*)	**100 %** n = 8 (7 ICR, 1 C57BL/6)	**4 %** ± 0.8 **n = 7 P = 0.02424 (6 ICR, 1 C57BL/6)	**Non-applicable** (there is no known morphological A-P axis)	EPC tilt aligned with: 1. **long** epiblast diameter: **100 %**, n = 6/6 (5 ICR, 1 C57BL/6) 2. **short** epiblast diameter: **0 %**, n = 0/6	**Non-applicable** (there is no known morphological A-P axis)
AVE-1 stage (*anterior visceral endoderm-1 stage*)	**100 %** n = 8 (3 ICR, 1 BALB/c, 4 C57BL/6)	**4.3 %** ± 1, n = 7, P = 0.8478 (3 ICR, 1 BALB/c, 3 C57BL/6)	A-P axis aligned with: 1. **long** epiblast diameter: **100 %**, n = 7/7 (3 ICR, 1 BALB/c, 3 C57BL/6) 2. **short** epiblast diameter: **0 %**, n = 0/7	EPC tilt aligned with: 1. **long** epiblast diameter: **100 %**, n = 7/7 (3 ICR, 1 BALB/c, 3 C57BL/6) 2. **short** epiblast diameter: **0 %**, n = 0/7	1. EPC tilt (for **AVE-1** stage) aligned with **A-P axis**: **100 %**, n = 7/7 (3 ICR, 1 BALB/c, 3 C57BL/6) 2. In embryos where EPC tilt and A-P axis are aligned (for **AVE-1 and AVE-2 combined**): EPC is tilted towards (a) **posterior** end: **53.3 %**, n = 8/15 (4 ICR, 2 BALB/c, 2 C57BL/6) (b) **anterior** end: **46.7 %**, n = 7/15 (4 ICR, 1 BALB/c, 2 C57BL/6)
AVE-2 stage (*anterior visceral endoderm-2 stage*)	**100 %** n = 16 (10 ICR, 3 BALB/c, 3 C57BL/6)	**4.4 %** ± 0.6 n = 16 P = 0.8672 (10 ICR, 3 BALB/c, 3 C57BL/6)	A-P axis aligned with: 1. **long** epiblast diameter: **100 %**, n = 16/16 (10 ICR, 3 BALB/c, 3 C57BL/6) 2. **short** epiblast diameter: **0 %**, n = 0/16	EPC tilt aligned with: 1. **long** epiblast diameter: **100 %**, n = 8/8 (5 ICR, 2 BALB/c, 1 C57BL/6) 2. **short** epiblast diameter: **0 %**, n = 0/8	1. EPC tilt (for **AVE-2** stage) aligned with **A-P axis**: **100 %**, n = 8/8 (5 ICR, 2 BALB/c, 1 C57BL/6) 2. In embryos where EPC tilt and A-P axis are aligned (for **AVE-1 and AVE-2 combined**): EPC is tilted towards (a) **posterior** end: **53.3 %**, n = 8/15 (4 ICR, 2 BALB/c, 2 C57BL/6) (b) **anterior** end: **46.7 %**, n = 7/15 (4 ICR, 1 BALB/c, 2 C57BL/6)
AVE-3 stage (*anterior visceral endoderm-3 stage*)	**100 %** n = 14 (12 ICR, 2 BALB/c)	**3.9 %** ± 0.8 n = 10 P = 0.6538 (8 ICR, 2 BALB/c)	A-P axis aligned with: 1. **long** epiblast diameter: **71 %**, n = 10/14 (9 ICR, 1 BALB/c) 2. **short** epiblast diameter: **29 %**, n = 4/14 (3 ICR, 1 BALB/c)	EPC tilt aligned with: 1. **long** epiblast diameter: **38.5 %**, n = 5/13 (5 ICR) 2. **short** epiblast diameter: **61.5 %**, n = 8/13 (6 ICR, 2 BALB/c)	1. EPC tilt (for **AVE-3** stage) aligned with **A-P axis**: **69.2 %**, n = 9/13 (8 ICR, 1 BALB/c) 2. In embryos where EPC tilt and A-P axis are aligned (for **AVE-3**): EPC is tilted towards (a) **posterior** end: **44.4 %**, n = 4/9 (3 ICR, 1 BALB/c) (b) **anterior** end: **55.6 %**, n = 5/9 (5 ICR)

(*continued on next page*)

Table-1 (*continued*)

	Parameters measured in live embryos (apply to ICR, BALB/c and C57BL/6 stains) Terms in *underlined italics* are explained in Supplementary Fig. 1				
Pre-streak stage (*pre-streak stage*)	**100 %** n = 38 (26 ICR, 2 BALB/c, 10 C57BL/6)	**8.7 %** ± 1 **n = 28 P = 0.007231 (16 ICR, 2 BALB/c, 10 C57BL/6)	A-P axis aligned with: 1. **long** epiblast diameter: **59.5 %**, n = 25/42 (19 ICR, 1 BALB/c, 5 C57BL/6) 2. **short** epiblast diameter: **40.5 %,** n = 17/42 (11 ICR, 1 BALB/c, 5 C57BL/6)	EPC tilt aligned with: 1. **long** epiblast diameter: **36.4 %**, n = 8/22 (8 ICR) 2. **short** epiblast diameter: **63.6 %,** n = 14/22 (10 ICR, 4 C57BL/6)	1. EPC tilt (for **pre-streak** stage) aligned with **A-P axis**: **86.4 %,** n = 19/22 (16 ICR, 3 C57BL/6) 2. In embryos where EPC tilt and A-P axis are aligned (for **pre-streak**): EPC is tilted towards (a) **posterior** end: **84.2 %,** n = 16/19 (13 ICR, 3 C57BL/6) (b) **anterior** end: **15.8 %,** n = 3/19 (3 ICR)
NS-1 stage (*nascent streak-1 stage*)	**100 %** n = 31 (28 ICR, 3 C57BL/6)	**12.7 %**±1.8* n = 12 P = 0.09759 (9 ICR, 3 C57BL/6)	A-P axis aligned with: 1. **long** epiblast diameter: **58 %**, n = 18/31 (17 ICR, 1 C57BL/6) 2. **short** epiblast diameter: **42 %,** n = 13/31 (11 ICR, 2 C57BL/6)	EPC tilt aligned with: 1. **long** epiblast diameter: **61.5 %**, n = 8/13 (8 ICR) 2. **short** epiblast diameter: **38.5 %,** n = 5/13 (4 ICR, 1 C57BL/6)	1. EPC tilt (for **NS-1** stage) aligned with **A-P axis**: **85 %,** n = 11/13 (10 ICR, 1 C57BL/6) 2. In embryos where EPC tilt and A-P axis are aligned (for **NS-1**): EPC is tilted towards (a) **posterior** end: **73 %,** n = 8/11 (8 ICR) (b) **anterior** end: **27 %,** n = 3/11 (2 ICR, 1 C57BL/6)
NS-2 stage (*nascent streak-2 stage*)	**100 %** n = 16 (13 ICR, 1 BALB/c, 2 C57BL/6)	**15.2 %** ± 3.2 n = 10 P = 0.6425 (7 ICR, 1 BALB/c, 2 C57BL/6)	A-P axis aligned with: 1. **long** epiblast diameter: **100 %**, n = 16/16 (13 ICR, 1 BALB/c, 2 C57BL/6) 2. **short** epiblast diameter: **0 %,** n = 0/16	EPC tilt aligned with: 1. **long** epiblast diameter: **87.5 %**, n = 7/8 (5 ICR, 2 C57BL/6) 2. **short** epiblast diameter: **12.5 %,** n = 1/8 (1 ICR)	1. EPC tilt (for **NS-2** stage) aligned with **A-P axis**: **87.5 %,** n = 7/8 (5 ICR, 2 C57BL/6) 2. In embryos where EPC tilt and A-P axis are aligned (for **NS-2 and ES combined**): EPC is tilted towards (a) **posterior** end: **50 %,** n = 6/12 (3 ICR, 3 C57BL/6) (b) **anterior** end: **50 %,** n = 6/12 (4 ICR, 2 C57BL/6)
ES stage (*early streak stage*)	**100 %**, n = 19 (16 ICR, 3 C57BL/6)	**25.6 %** ±7.7 **n = 10 P = 0.01121 (7 ICR, 3 C57BL/6)	A-P axis aligned with: 1. **long** epiblast diameter: **100 %**, n = 21/21 (18 ICR, 3 C57BL/6) 2. **short** epiblast diameter: **0 %,** n = 0/21	EPC tilt aligned with: 1. **long** epiblast diameter: **100 %**, n = 5/5 (2 ICR, 3 C57BL/6) 2. **short** epiblast diameter: **0 %,** n = 0/5	1. EPC tilt (for **ES** stage) aligned with **A-P axis**: **100 %,** n = 5/5 (2 ICR, 3 C57BL/6) 2. In embryos where EPC tilt and A-P axis are aligned (for **NS-2 and ES combined**): EPC is tilted towards (a) **posterior** end: **50 %,** n = 6/12 (3 ICR, 3 C57BL/6) (b) **anterior** end: **50 %,** n = 6/12 (4 ICR, 2 C57BL/6)

pre-DVE and ES stages where the expression of *Bra* and *Cer* were previously shown to be absent or present, respectively [16,26] (Fig. 2, SupplTable-2). Briefly, AVE-1-3 stages are new subdivisions of the reported laterodistal VET stage [17], with AVE-1 being the earliest stage when A-P axis appears, as it represents the earliest asymmetry in VET location (explained in Suppl.Fig. 1 and SupplTable-1 and shown in Figs. 1 and 2) detected in embryo side-views: embryo orientation where both posterior and anterior ends/sides of A-P axis are morphologically identifiable on opposite sides in the same embryo image (Figs. 1 and 2, SupplTable-1,Suppl.Fig. 1). We also morphologically identified for the first time the gastrulation initiation stage [25–27], named here nascent streak (NS), based on opacity (explained in Suppl.Fig. 1) detected on one side of proximal embryonic region in side-views of pre-mesoderm embryos, which coincided with pre-mesoderm epiblast *Bra* expression (Figs. 1 and 2, SupplTable-1,Suppl.Fig. 1). This opacity originates from embVE, as this was the only opaque tissue when this part of embryonic region was micro-surgically separated into its constituent epiblast and embVE (Suppl.Fig. 2). We subdivided the NS stage into NS-1 and NS-2 based on the maximum limit of the distal end of this opacity, which coincides with that of *Bra*.Specifically, this limit is more proximally located in NS-1 embryos, signifying shorter streak length at NS-1 than at NS-2 stage (Figs. 1 and 2, SupplTable-1,Suppl.Fig. 1). Additionally, we identified a pre-streak stage between AVE-3 and NS-1, which may be analogous to the reported lateral/proximo-lateral VET stage [17] (Figs. 1 and 2,SupplTable-1,Suppl.Fig. 1). These results indicate that pre-ES embryos can be staged with more precision than before and identify the stages when the A-P axis initiates (AVE-1 and AVE-2) and when gastrulation begins (NS-1 and NS-2).

We used our more refined staging to examine the unresolved orientation of A-P axis in relation to the long and short epiblast diameters [17] from pre-DVE to ES stages, as explained in SupplTable-1/Suppl. Fig. 1. *First*, as reported [7], we confirm that the epiblast is bilaterally symmetric throughout this period since each embryo has a long and a short epiblast diameter at all stages analysed (Fig. 1,Table-1). *Second*, contrary to previous interpretations [2,7,16,17], when the A-P axis initiates (at our AVE-1/2 stages), it more aligns with the long epiblast diameter (n = 23/23) (Figs. 1 and 2,Table-1), in agreement with all other eutherian pre-gastrulation embryos examined including humans [9–14]. This suggests that the poorly understood factors responsible of aligning the newly formed mouse A-P axis are spatially related to the long, rather than the short, epiblast diameter. It also offers an alternative hypothesis for why gene-knockout embryos that fail to align their A-P axis with the long epiblast diameter by the ES stage [18–21]. That is, they fail to do so because they may fail to initially align this axis with the long epiblast diameter in the first place, rather than, as current thinking goes, due to failure to convert an initially aligned A-P axis with the short diameter to one aligned with the long diameter [18–21]. *Third*, at AVE-3, pre-streak and NS-1 stages, most embryos maintain their initial A-P axis orientation [n = 10/14 (71 %), n = 25/42 (60 %) and n = 18/31 (58 %), respectively] but some change it, as it aligns with the short epiblast diameter (29 %, 40 % and 42 % of embryos at AVE-3, pre-streak and NS-1, respectively) (Fig. 1,Table-1). Although this disagrees with previous interpretations [7,16,17], it agrees with them in that the A-P axis in pre-mesoderm embryos aligns with either the long or the short

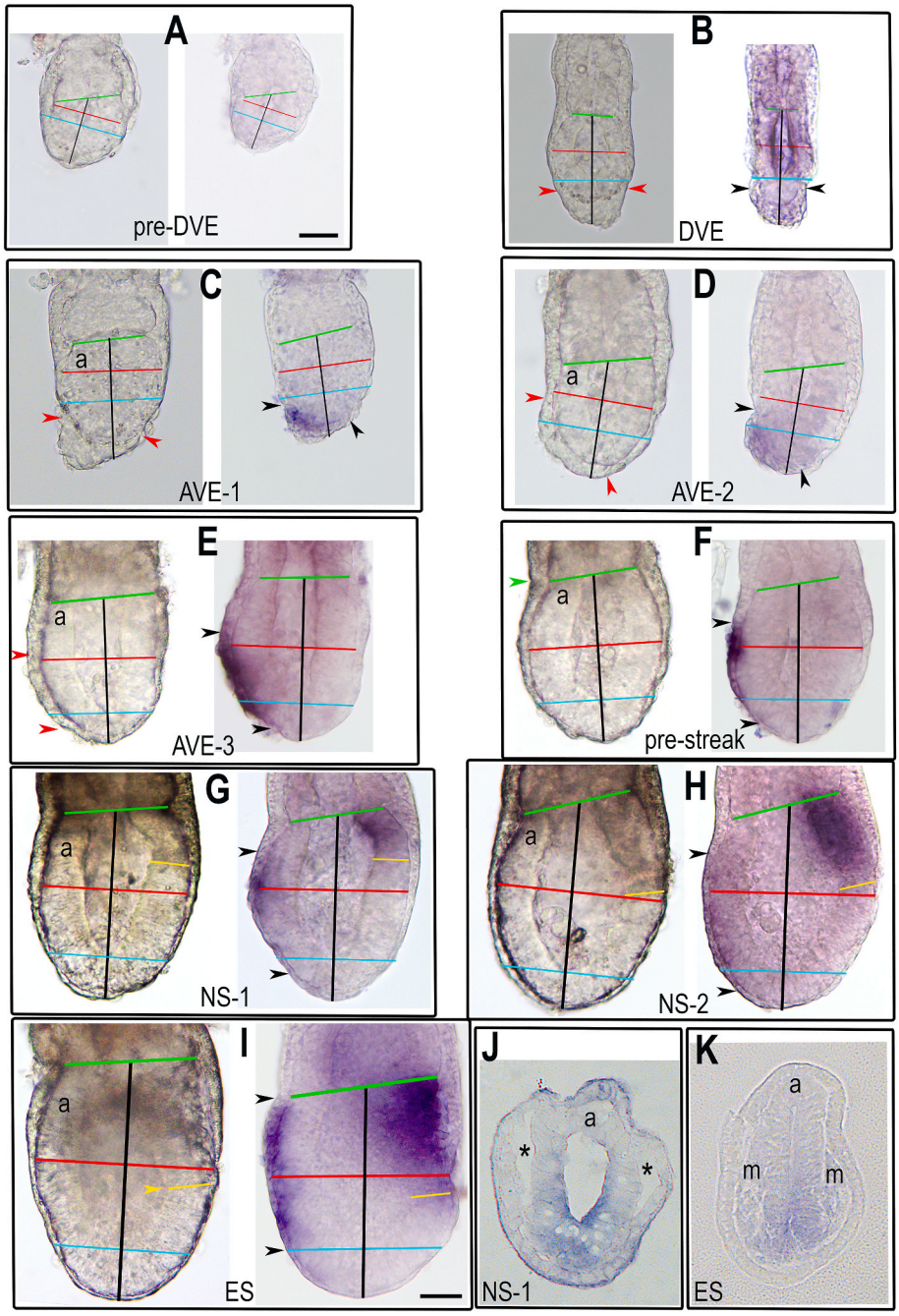

Fig. 2. *Molecular validation of 'A-P axis orientation/polarity' and embryo staging, based on comparing live 'embryo side-views' with Bra and Cer expression patterns.* (A–I): Each panel shows 'embryo side views' of same embryo live (left) and after double WISH for *Bra* and *Cer* (right), which when expressed (blue signal) mark posterior epiblast and DVE/AVE, respectively. Note that: (a) *Bra* and *Cer* are not expressed in pre-DVE (A), (b) *Bra* is expressed from NS-1 onwards and coincides with 'asymmetric opacity in proximal embryonic region' (G–I), (c) *Cer* coincides with 'VET' of DVE and AVE-1 to AVE-3 (B–E) and also marks AVE at stages where VET (as defined here) is not a staging criterion (F–I). (J, K): Cryo-sections of proximal 'embryonic region' that are perpendicular to the 'P-D axis' at NS-1 (J) and ES (K) stages of WISH embryos for *Bra/Cer* and *Bra* expression, respectively. Note that in NS-1 embryos *Bra* is expressed before mesoderm formation (J) and at ES marks both EMT epiblast and newly formed mesoderm (K). For explanation of stages and terms in inverted commas, see main text, Suppl.Fig. 1 and SupplTable-1. Panels A–H and J are at same magnification, as are panels I and K, (scale bars in A and I are 100 μm). Symbols and letters: as in legend of Fig. 1. Additionally: black arrowheads, borders of *Cer* expression domain; * empty space artifact between epiblast and embVE due to cryo-sectioning.

epiblast diameter. A reason why some embryos change their initial A-P axis orientation by AVE-3/pre-streak/NS-1 could be because they are those that fail to sufficiently grow, since embryos from this period whose A-P axis is aligned with short epiblast diameter, have a smaller egg cylinder length [16]. *Fourth*, we identified the NS-2 stage as the previously unknown stage closest to the ES stage when all embryos align their A-P axis with the long epiblast diameter (n = 16/16), thereby showing for the first time that this stage occurs during gastrulation but not before it as previously thought (Figs. 1 and 2,Table-1). This orientation was also seen in all embryos at ES stage (n = 21/21) (Figs. 1 and 2,Table-1), in agreement with published findings [15], thereby validating our methodology for identifying A-P axis orientation as we used the ES stage as a positive control for this. We speculate that if AVE-3/pre-streak/NS-1 embryos that align their A-P axis with short epiblast diameter are

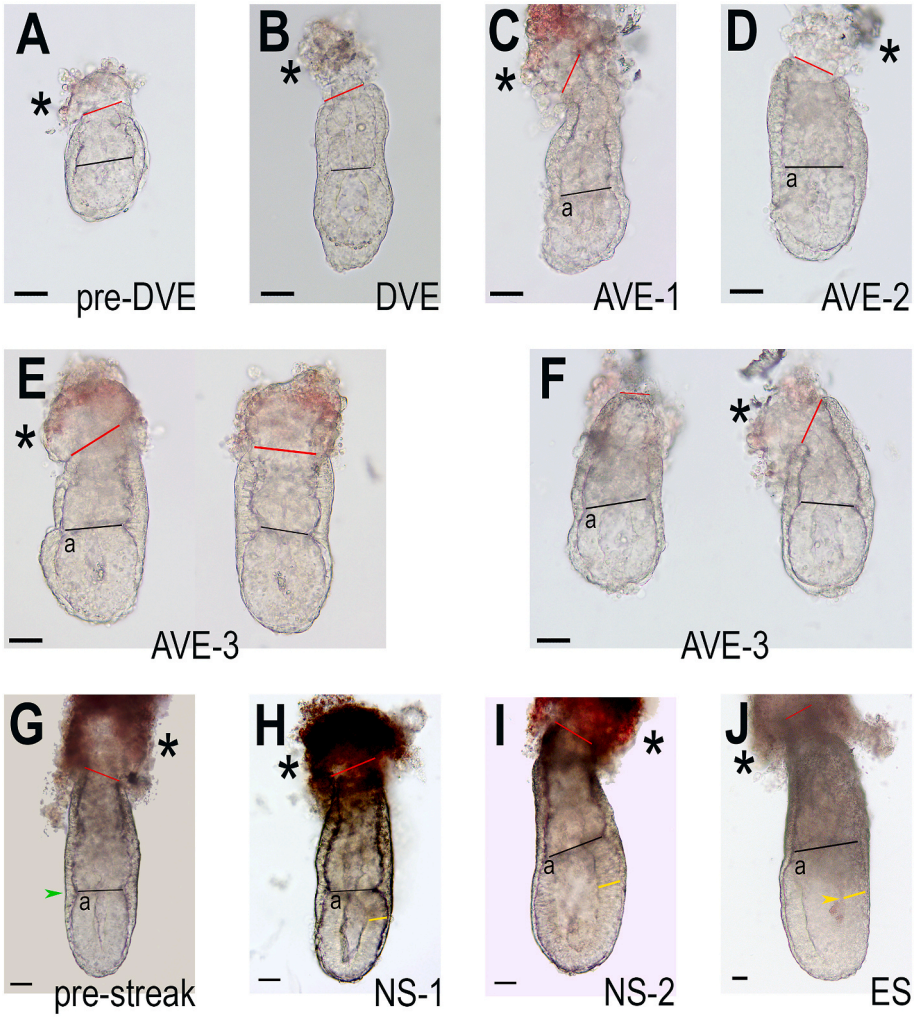

Fig. 3. *'EPC tilt orientation/polarity' in relation to those of 'A-P axis' from pre-DVE to ES stages*. Live embryos imaged from their long (A-D, E/F left images, I and J) or short (E/F right images, G and H) epiblast diameter sides, before or after A-P axis formation (A/B and C-J, respectively). (C, D, left images in E/F, G-J): 'embryo side-views' which coincide with 'A-P axis orientation'. (right images in E/F): 'embryo orthogonal views', which are at right angles to A-P axis orientation. Examples of embryos where 'EPC tilt' orientation is more aligned with: (a) 'long epiblast diameter' in pre-DVE and DVE embryos (A, B), (b) orientation of A-P axis (C, D, G-J, and left image in E), and (c) orientation orthogonal to A-P axis (right image in F). Examples of embryos where EPC is tilted towards the anterior (C, left image in E, H, J) or posterior (D, G, I) sides of A-P axis. For explanation of stages and terms in inverted commas, see main text, Suppl.Fig. 1 and SupplTable-1. Panels A–F are at same magnification, as are G-I (scale bars are 100 μm). Symbols and letters: *, side towards which EPC is tilted; a, anterior end of epiblast (only in embryos with A-P axis); red line, 'ExE-EPC junction' denoting orientation of 'EPC tilt'; black line, 'epiblast-ExE junction'; green arrowhead, dent in VE (anterior side in the vicinity of epiblast-EXE junction) in pre-streak embryos; yellow line, distal end of 'asymmetric opacity in proximal embryonic region'; yellow arrowhead, 'distal end of mesodermal wings'.

those that are growth retarded [16], a a possible cause for realignment of their A-P axis with the long diameter by NS-2/ES stages could be their compensatory growth (part of embryo size regulation), which in post-implantation embryos commences at around this time [35]. Therefore, our results provide evidence that, contrary to current belief, the A-P axis in pre-ES embryos is predominantly aligned with the long, rather then the short, epiblast diameter.

EPC tilt orientation and polarity were identified using previously described criteria [15,29–32] as explained in the text and Suppl.Fig. 1 and shown in Fig. 3. The ES stage was used as a positive control for validating our methodology for identifying EPC tilt orientation and polarity. This is because our results for the ES stage are in agreement with what was previously shown at this stage (Fig. 3,Table-1): the orientation of this tilt is aligned with that of the A-P axis and the long epiblast diameter whilst its polarity is random [15]. Regarding the unknown relationship between the polarity and orientation of the EPC tilt and to those of the A-P axis and the long and short epiblast diameters in pre-ES embryos, we show for the first time the following. *First*, before A-P axis formation at pre-DVE/DVE and during A-P axis initiation at AVE-1/2, the EPC tilt aligns with the long epiblast diameter (n = 10/10 at pre-DVE/DVE and n = 15/15 at AVE-1/2) and coincides with the orientation of the newly formed A-P axis (n = 15/15 at AVE-1/2). However, the polarity of the EPC tilt in relation to that of the newly-formed A-P axis at AVE-1/2 stages, is apparently random, as it was tilted towards the posterior or anterior sides of this axis at approximately equal frequencies: 53.3 % (n = 8/15) towards the posterior and 46.7 % (n = 7/15) towards the anterior (Fig. 3,Table-1). This novel association of EPC tilt orientation with the long epiblast diameter before A-P axis formation at pre-DVE/DVE stages, and with both this diameter and A-P axis orientation when this axis initiates at AVE-1/2 stages, implicates the orientation of this trophoblast asymmetry as a possible guiding factor of A-P axis orientation. The lack of association between EPC tilt polarity and that of A-P axis at AVE1/2 stages excludes the former from being involved in the latter and is consistent with previously findings at the ES stage [15]. *Second*, during the AVE-3, pre-streak and NS-1 stages where 30 %–40 % of embryos have their

A-P axis more aligned with the short epiblast diameter (Fig. 1,Table-1), the orientation of EPC tilt was more aligned with that of A-P axis in most embryos: detected in about 70 % (n = 9/13), 86 % (n = 19/22) and 85 % (n = 11/13) of embryos at AVE-3, pre-streak and NS-1 stages, respectively (Fig. 1,Table-1). *Third*, similar to what was documented for ES embryos [15] and what we observed at the AVE-1/2 period, we found that by the NS-2/ES stages where A-P axis is more aligned with the long epiblast diameter (Fig. 1,Table-1): (a) the orientation of EPC tilt is more aligned with that of the A-P axis (n = 7/8 at NS-2 and n = 5/5 at ES stages), and (b) the directionality of this tilt is random [50 % (n = 6/12) towards the posterior and 50 % (n = 6/12) towards the anterior] (Fig. 1, Table-1). Collectively, our results implicate the orientation of the EPC tilt as a possible factor for orientating the A-P axis since this tilt exists before A-P axis initiation and its orientation coincides with that of the A-P axis in all embryos at AVE-1, AVE-2, almost all at NS-1 and NS-2 and most of them at AVE-3 and pre-streak stages.

In conclusion, we established a more refined embryo staging between the well-established pre-DVE/DVE and ES stages which provides live morphological criteria for identifying the previously unidentified stages when A-P axis initiates (AVE-1) and gastrulation begins (NS-1). Importantly, we used this staging in pre-ES embryos to identify hitherto unresolved aspects of A-P axis orientation in relation to the long and short diameters and to elucidate the unknown relationship between the orientation of this axis and that of the EPC tilt. These new findings lead to alternative explanations about mouse A-P axis orientation and implicate a specific trophoblast asymmetry as a possible determining factor in orientating this axis when it first forms.

CRediT authorship contribution statement

Xenia Hadjikypri: Methodology, Investigation, Data curation. **Christina Theofanous:** Methodology, Investigation, Formal analysis, Data curation. **Antonia Christodoulidi:** Methodology, Investigation, Formal analysis. **Pantelis Georgiades:** Writing – review & editing, Writing – original draft, Validation, Supervision, Project administration, Formal analysis, Conceptualization.

Declaration of competing interest

The authors declare that they have no known competing financial interests or personal relationships that could have appeared to influence the work reported in this paper.

Acknowledgments

This work was funded by the University of Cyprus.

Appendix A. Supplementary data

Supplementary data to this article can be found online at https://doi.org/10.1016/j.bbrep.2024.101817.

References

[1] R.S. Beddington, E.J. Robertson, Axis development and early asymmetry in mammals, Cell 96 (1999) 95–209.
[2] A. Perea-Gomez, S.M. Meilhac, Formation of the anterior-posterior axis in mammals, in: Principles of Developmental Genetics, Academic Press, 2015, pp. 171–188.
[3] G. Peng, S. Suo, G. Cui, et al., Molecular architecture of lineage allocation and tissue organization in early mouse embryo, Nature 572 (2019) 528–532.
[4] J. Zhai, Z. Xiao, Y. Wang, et al., Human embryonic development: from peri-implantation to gastrulation, Trends Cell Biol. 32 (2022) 18–29.
[5] S. Ghimire, V. Mantziou, N. Moris, et al., Human gastrulation: the embryo and its models, Dev. Biol. 474 (2021) 100–108.
[6] K.M. Downs, T. Davies, Staging of gastrulating mouse embryos by morphological landmarks in the dissecting microscope, Development 118 (1993) 1255–1266.
[7] D. Mesnard, M. Filipe, J.A. Belo, et al., The anterior-posterior axis emerges respecting the morphology of the mouse embryo that changes and aligns with the uterus before gastrulation, Curr. Biol. 14 (2004) 184–196.
[8] J.A. Rivera-Pérez, A.K. Hadjantonakis, The dynamics of morphogenesis in the early mouse embryo, Cold Spring Harbor Perspect. Biol. 7 (2015) a015867.
[9] C. Viebahn, C. Stortz, S.A. Mitchell, et al., Low proliferative and high migratory activity in the area of Brachyury expressing mesoderm progenitor cells in the gastrulating rabbit embryo, Development 129 (2002) 2355–2365.
[10] R. Plöger, C. Viebahn, Expression patterns of signalling molecules and transcription factors in the early rabbit embryo and their significance for modelling amniote axis formation, Dev. Gene. Evol. 231 (2021) 73–83.
[11] R. Hassoun, P. Schwartz, K. Feistel, et al., Axial differentiation and early gastrulation stages of the pig embryo, Differentiation 78 (2009) 301–311.
[12] J. van Leeuwen, D.K. Berg, P.L. Pfeffer, Morphological and gene expression changes in cattle embryos from hatched blastocyst to early gastrulation stages after transfer of in vitro produced embryos, PLoS One 10 (2015) e0129787.
[13] M.A. Molè, T.H. Coorens, M.N. Shahbazi, et al., A single cell characterisation of human embryogenesis identifies pluripotency transitions and putative anterior hypoblast centre, Nat. Commun. 12 (2021) 3679.
[14] R. O'Rahilly, The manifestation of the axes of the human embryo, Z. Anat. Entwicklungsgeschichte 132 (1970) 50–57.
[15] R.L. Gardner, M.R. Meredith, D.G. Altman, Is the anterior-posterior axis of the fetus specified before implantation in the mouse? J. Exp. Zool. 264 (1992) 437–443.
[16] A. Perea-Gomez, A. Camus, A. Moreau, et al., Initiation of gastrulation in the mouse embryo is preceded by an apparent shift in the orientation of the anterior-posterior axis, Curr. Biol. 14 (2004) 197–207.
[17] J.A. Rivera-Pérez, J. Mager, T. Magnuson, Dynamic morphogenetic events characterize the mouse visceral endoderm, Dev. Biol. 261 (2003) 470–487.
[18] Q. Guo, J.Y. Li, Distinct functions of the major Fgf8 spliceform, Fgf8b, before and during mouse gastrulation, Development 134 (2007) 2251–2260.
[19] J.R. Barrow, W.D. Howell, M. Rule, et al., Wnt3 signaling in the epiblast is required for proper orientation of the anteroposterior axis, Dev. Biol. 312 (2007) 312–320.
[20] G.G. Tortelote, J.M. Hernández-Hernández, A.J. Quaresma, et al., Wnt3 function in the epiblast is required for the maintenance but not the initiation of gastrulation in mice, Dev. Biol. 374 (2013) 164–173.
[21] Y. Yoon, T. Huang, G.G. Tortelote, et al., Extra-embryonic Wnt3 regulates the establishment of the primitive streak in mice, Dev. Biol. 403 (2015) 80–88.
[22] B.J. Poland, J.R. Miller, M. Harris, et al., Spontaneous abortion: a study of 1,961 women and their conceptuses, Acta Obstet. Gynecol. Scand. 60 (1981) 3–32.
[23] J.A. Rivera-Pérez, V. Jones, P.P. Tam, Culture of whole mouse embryos at early postimplantation to organogenesis stages: developmental staging and methods, in: Methods in Enzymology, Academic Press, 2010, pp. 185–203.
[24] K.A. Lawson, V. Wilson, A revised staging of mouse development before organogenesis, in: Kaufman's Atlas of Mouse Development Supplement, Academic Press, 2016, pp. 51–64.
[25] K. Hashimoto, N. Nakatsuji, Formation of the primitive streak and mesoderm cells in mouse embryos—detailed scanning electron microscopical study, Dev. Growth Differ. 31 (1989) 209–218.
[26] S.M. Morgani, J.J. Metzger, J. Nichols, et al., Micropattern differentiation of mouse pluripotent stem cells recapitulates embryo regionalized cell fate patterning, Elife 7 (2018) e32839.
[27] S.M. Morgani, A.K. Hadjantonakis, Signaling regulation during gastrulation: insights from mouse embryos and in vitro systems, Curr. Top. Dev. Biol. 137 (2020) 391–431.
[28] M. Williams, C. Burdsal, A. Periasamy, et al., Mouse primitive streak forms in situ by initiation of epithelial to mesenchymal transition without migration of a cell population, Dev. Dynam. 241 (2012) 270–283.
[29] L.J. Smith, Embryonic axis orientation in the mouse and its correlation with blastocyst relationships to the uterus: II. Relationships from 4¼ to 9½ days, Development 89 (1985) 15–35.
[30] J. Rossant, P.P. Tam, Emerging asymmetry and embryonic patterning in early mouse development, Dev. Cell 7 (2004) 155–164.
[31] J. Rossant, P.P. Tam, Blastocyst lineage formation, early embryonic asymmetries and axis patterning in the mouse, Development 136 (2009) 701–713.
[32] S. Nikolaou, X. Hadjikypri, G. Ioannou, et al., Functional and phenotypic distinction of the first two trophoblast subdivisions and identification of the border between them during early postimplantation: a prerequisite for understanding early patterning during placentogenesis, Biochem. Biophys. Res. Commun. 496 (2018) 64–69.
[33] C. Polydorou, P. Georgiades, Ets2-dependent trophoblast signalling is required for gastrulation progression after primitive streak initiation, Nat. Commun. 4 (2013) 1–13.
[34] A. Nagy, M. Gertsenstein, K. Vintersten, et al., Manipulating the Mouse Embryo: a Laboratory Manual, Cold Spring Harbor Laboratory Press, 2003.
[35] M.A. Power, P.P. Tam, Onset of gastrulation, morphogenesis and somitogenesis in mouse embryos displaying compensatory growth, Anat. Embryol. 187 (1993) 493–504.